Available online at www.sciencedirect.com
SCIENCE DIRECT®
Journal of Photochemistry and Photobiology A: Chemistry 160 (2003) 47–53
Journal of Photochemistry and Photobiology A:Chemistry
www.elsevier.com/locate/jphotochem

Active sites on silica-supported zirconium oxide for photoinduced direct methane conversion and photoluminescence

H. Yoshida [a,*], M.G. Chaskar [a,b], Y. Kato [a], T. Hattori [a]

[a] *Department of Applied Chemistry, Graduate School of Engineering, Nagoya University, Furo-cho Chikusa-ku, Nagoya 464-8603, Japan*
[b] *Department of Chemistry, Annasaheb Mager College, Pune District Education Association, Pune 4110028, India*

Received 16 December 2002; received in revised form 21 February 2003; accepted 10 April 2003

Abstract

Photoactivity of silica-supported zirconium oxide (ZrO_2/SiO_2) of low loading below 1 mol% for photoinduced direct methane conversion at room temperature was examined. Very low loading samples below 0.1 mol% exhibited high activity for methane coupling upon photoirradiation. The highly dispersed Zr oxide species on the silica surface had different electronic and local structure from ZrO_2 particles, and exhibited fine structural phosphorescence spectra. From the fine structure, it was revealed that the highly dispersed zirconium oxide species have photoactive Zr–O–Si linkage whose vibration energy was estimated to be 955 cm^{-1}. From the decay curve analysis and quenching experiment, it is proposed that the Zr species have around 28 ± 5 ms of excitation lifetime at 77 K and they are responsible for the photoinduced direct methane coupling at room temperature.

Keywords: Silica-supported zirconium oxide; Photoluminescence; Methane; Photoinduced direct methane conversion; Photocatalysis

1. Introduction

In order to make an efficient utilization of natural gas, we must consider transforming it to more valuable chemicals. Higher hydrocarbons such as ethane, ethene and so on are more useful for chemical industry than methane. When two methane molecules react directly, hydrogen and higher hydrocarbons such as ethane can be obtained as follows:

$$2CH_4 \rightarrow C_2H_6 + H_2, \quad \Delta G\,(298\,K) = 68.6\,kJ/mol \qquad (1)$$

The large and positive ΔG value implies that the reaction hardly proceeds at mild condition.

The oxidative coupling of methane (OCM) seems the effective reaction for producing higher hydrocarbons and has been extensively studied worldwide since the formation of water reduces the potential of products. However, no catalysts could reach the principal criteria for industrial application of OCM [1], since it is quite difficult to obtain the coupling products in high yield with less CO_x formation. The limits of the process have been essentially indicated [2].

Photocatalytic system has potential to promote difficult reactions. Several researchers have examined both oxidative [3] and non-oxidative [4–6] photoinduced systems for methane conversion. In both systems, however, the performance was not sufficient; in the oxidative system employing TiO_2 photocatalyst the complete oxidation mainly occurred [3], while the conversion of methane was extremely low in non-oxidative systems employing V/SiO_2 [4], TiO_2 [5] and Mo/SiO_2 [6]. Recently, it was found that silica–alumina [7–9] and zeolites [10] exhibited the activity for methane conversion upon photoirradiation to produce higher hydrocarbons and hydrogen. And silica–alumina–titania system [11] showed much higher catalytic activity for this photoinduced direct methane coupling. To our knowledge, this was the first report in which photocatalytic direct methane coupling was confirmed. However, the sufficient activity has not been attained yet. Thus, the discovery of novel suitable photocatalytic systems as well as some directions for intelligent catalyst design are still required.

Zirconium oxide is known as a semiconductor exhibiting photocatalytic activity for oxidation [12,13] and water decomposition [14]. As for dispersed zirconium oxide species on/in silica, the photocatalytic properties have not been revealed except for only a few systems such as photodegradation of 4-nitrophenol [15], photoisomerization of 2-butene [16]. In the present study, we prepared silica-supported zirconium oxide of low Zr content from 0.01 to 1.0 mol%, and examined their photocatalytic activity for the direct

* Corresponding author. Tel.: +81-52-789-4609; fax: +81-52-789-3193.
E-mail address: yoshidah@apchem.nagoya-u.ac.jp (H. Yoshida).

1010-6030/03/$ – see front matter © 2003 Elsevier Science B.V. All rights reserved.
doi:10.1016/S1010-6030(03)00220-X

methane conversion at room temperature. In addition, we characterized the samples by using some spectroscopies such as XANES, UV and photoluminescence, to clarify the photoactive sites.

2. Experimental

2.1. Sample preparation

Amorphous silica was prepared from $Si(OEt)_4$ by sol–gel method, followed by calcination in a flow of air at 773 K for 5 h [17]. BET surface area of the silica was 679 $m^2\,g^{-1}$. Silica-supported zirconium oxide samples were prepared by impregnation method [18]: amorphous silica was impregnated by aqueous solution of zirconyl nitrate dehydrate, dried at 383 K for overnight (12 h) and calcined at 773 K in a flow of dry air for 5 h. The prepared silica-supported zirconium oxide samples are referred to as $ZrO_2/SiO_2(x)$, where x is molar ratio: $x = N_{Zr}/(N_{Zr} + N_{Si}) \times 100$ (mol%), N_M is the number of M atoms in the sample. Zirconium oxide sample employed for the photoinduced reaction and UV spectrum experiments was commercially obtained (Kishida) and the BET surface area was 7.0 $m^2\,g^{-1}$ after calcination at 1073 K. Another zirconium oxide samples employed for the XAFS spectroscopy was obtained by calcination of zirconium hydroxide (Wako) at 723 or 1073 K.

2.2. Photocatalytic test

The reaction tests were carried out using a closed quartz reactor (82 cm^3) as illustrated in Fig. 1 in a similar way to the previous studies [7–11]. The powder sample (0.5 g) was spread on the flat bottom of the reactor (19.6 cm^2) and was treated with 60 Torr (8.0 kPa) oxygen for 1 h at 1073 K, followed by evacuation for 1 h at 1073 K. Methane (99.95%) purchased was further purified by a vacuum evaporation before use and introduced into the reactor. The initial pressure of methane (200 μmol) in the reactor was 52 Torr (6.9 kPa) and no oxidant molecules were introduced. The sample was irradiated with a 250 W Xe lamp for 3 h. Under photoirradiation, the temperature of sample bed was measured to be ca. 305 K. Products in the gaseous phase were collected with a liquid-N_2 trap and analysed by gas chromatography (GC). Then desorption of adsorbed products were carried out by heating (573 K, 15 min), followed by collection and analysis by GC.

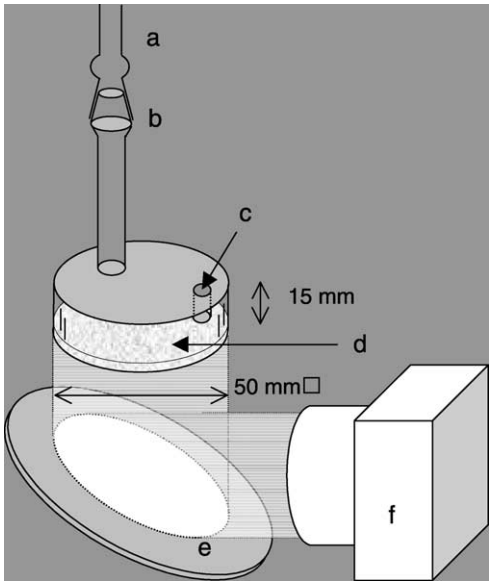

Fig. 1. Schematic drawing of the photoreactor: (a) a conventional vacuum line equipped with pressure gage, (b) joint, (c) small hole for thermo-couple, (d) catalyst bed, (e) UV-reflection mirror, (f) Xe lamp.

2.3. Characterization

Before recording the following spectra (XAFS, DR-UV-Vis, photoluminescence), the samples were treated with 60 Torr oxygen for 1 h at 1073 K, followed by evacuation for 1 h at 1073 K.

Zr K-edge XAFS spectra were recorded at the BL-10B station [19] at KEK-PF with a Si(3 1 1) channel cut monochromator at room temperature. The spectra of reference samples were recorded in transmission mode. Those of the samples were recorded in fluorescence mode by using Lytle detector [20] with a 100 mm chamber of Kr. The Sr-filter ($\mu t = 6$) was employed as Z-1 filter. The pretreated catalysts were sealed in polyethylene packs under nitrogen atmosphere without exposure to atmosphere.

Diffuse reflectance UV-Vis spectra were recorded on a JASCO V-570 equipped with an integrating sphere covered with $BaSO_4$. The sample was pretreated in the same way as mentioned above, and transferred to the optical cell in vacuo without exposure to atmosphere.

The phosphorescence spectra and decay curves were recorded with Hitachi F-4500 fluorescence spectrophotometer at 77 K with a UV-cut filter (transmittance >310 nm) to remove scattered light from the UV source (a Xe lamp), where the fluorescence emission was cut off electrically to record phosphorescence emission. The sample pretreated was transferred to the optical cell in vacuo without exposure to atmosphere.

3. Results and discussion

3.1. Photoinduced direct methane conversion

We examined the activity of SiO_2, ZrO_2 and the ZrO_2/SiO_2 samples in the photoinduced non-oxidative methane conversion, and the results are listed in Table 1. On the SiO_2 sample (Table 1, run 1), only a small amount of C_2H_6 was obtained in gas phase. The $ZrO_2/SiO_2(0.01)$ sample produced five times higher amount of C_2H_6 than SiO_2 did (run 2). A trace amount of C_2H_4 was also obtained as

thermally desorbed products. It is suggested that the zirconium species dispersed on silica would be responsible for the high activity for the methane conversion. On the ZrO_2/SiO_2(0.1) sample, C_3H_8 was also obtained in addition to C_2H_6 and a trace amount of C_2H_4 (run 3). This sample exhibited the highest activity among the samples examined in the present study, although it seemed lower than the activity of the silica–alumina–titania system that was the highest so far [11].

In the previous study on photoirradiated silica–alumina [7–9], zeolite [10] and silica–alumina–titania systems [11], it was confirmed that the methane was converted to higher hydrocarbons, such as ethane, ethene, propane, with almost stoichiometric production of hydrogen. In the present system and under the present condition, the formation of hydrogen was not confirmed. Although this might be due to too low conversion of methane to detect hydrogen, the possibility of oxidative methane coupling occurring could not be excluded at this moment.

Further increase of the zirconium amount more than 0.1 mol% reduced the products yield: the samples including 0.5 or 1.0 mol% of zirconium showed lower activity than the ZrO_2/SiO_2(0.01) sample and ZrO_2/SiO_2(0.1) sample did (Table 1, runs 4 and 5). It is speculated that the aggregated zirconium oxide species on silica have lower or no activity for this photoinduced direct methane conversion. On the zirconium oxide without silica-support, no products were obtained (Table 1, run 6). Although the specific surface area of this sample was quite low, the number of surface zirconium sites on this non-supported sample was estimated to be equivalent or superior to that on the supported samples, meaning that the bulk zirconium oxide obviously have less specific activity for this reaction than the dispersed zirconium species on silica have. This supports the above speculation that the lower activity of the ZrO_2/SiO_2(0.5) sample and ZrO_2/SiO_2(1.0) sample are due to aggregation of zirconium oxide species on silica surface. At the same time, it is suggested that the dispersed zirconium oxide species interacted with silica surface should exhibit the high activity for the photoinduced non-oxidative direct methane coupling.

Table 1
Results of photoinduced direct methane conversion[a]

Run	Sample	Product (C%)[b]			Total (C%)[b]
		C_2H_6	C_3H_8	C_2H_4 (desorbed)	
1	SiO_2	0.021	0	0	0.021
2	ZrO_2/SiO_2(0.01)	0.104	0	tr.	0.104
3	ZrO_2/SiO_2(0.1)	0.109	0.003	tr.	0.112
4	ZrO_2/SiO_2(0.5)	0.031	0	tr.	0.031
5	ZrO_2/SiO_2(1.0)	0.052	0	tr.	0.052
6	ZrO_2	0	0	0	0

[a] Reaction temperature = ca. 310 K, reaction time = 3 h, CH_4 = 200 μmol; sample = 0.5 g.
[b] Based on the initial amount of CH_4; tr. = trace.

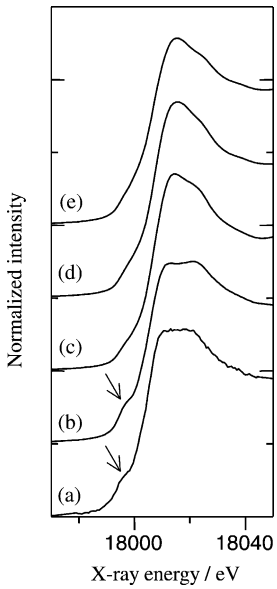

Fig. 2. Zr K-edge XANES spectra of ZrO_2/SiO_2(0.1) (a), ZrO_2/SiO_2(1.0) (b), Zr hydroxide (c), ZrO_2 (723 K) (d), ZrO_2 (1173 K) (e). The samples were pretreated at 1073 K and sealed.

3.2. Structure of zirconium species dispersed on silica

XANES spectrum reflects the local coordination symmetry of target atom. Fig. 2 shows Zr K-edge XANES spectra of the representative samples and reference samples. The spectra of ZrO_2/SiO_2 samples are obviously different from those of zirconium hydroxide and ZrO_2 samples on the feature of the post-edge feature as well as the pre-edge shoulder. It was clearly demonstrated that the local structure of zirconium oxide species dispersed on silica was quite different from those of bulk ZrO_2 and Zr hydroxide. These features have been also reported by Mountjoy et al. about ZrO_2–SiO_2 xerogel system [21]. The pre-edge feature (arrows in Fig. 2) is mainly due to 1s–4d transition, which is fundamentally forbidden transition. This appearance corresponds to p–d mixing due to asymmetric coordination state of zirconium oxide species. Mountjoy et al. proposed that the zirconium species exhibiting such pre-edge feature would be atomic dispersed in silica and have similar coordination symmetry to *n*-propoxide but with higher than 6-hold coordination [21]. The atomically dispersed zirconium should have strong interaction with silica, in other words, it is expected that there are Zr–O–Si bonds.

The electronic structure can be characterized by UV spectroscopy. Fig. 3 shows diffuse reflectance UV spectra of the samples evacuated at 1073 K. The SiO_2 sample showed a very small broad band (Fig. 3a), which is assignable to some kinds of surface defect sites [22,23]. The ZrO_2/SiO_2(0.01) sample showed a broad band below 350 nm, which maximum was centered around 240 nm (Fig. 3b), and the ZrO_2/SiO_2(0.1) sample showed more intense band at the same region (Fig. 3c). This band feature disappeared (or much reduced) on the spectra of the samples of larger

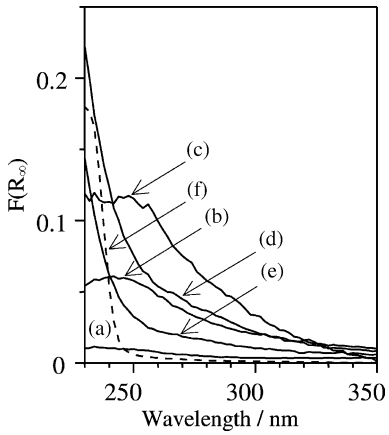

Fig. 3. Diffuse reflectance UV spectra of SiO_2 (a), ZrO_2/SiO_2(0.01) (b), ZrO_2/SiO_2(0.1) (c), ZrO_2/SiO_2(0.5) (d), ZrO_2/SiO_2(1.0) (e), and ZrO_2 (f). The intensity of curve f was reduced to 1/10. $F(R_\infty)$ is Kubelka-Munk function.

zirconium content, ZrO_2/SiO_2(0.5) and ZrO_2/SiO_2(1.0), which showed only a large band at shorter wavelength (Fig. 3d and e). The bulk ZrO_2 showed much larger band (the intensity in Fig. 3f was reduced to one-tenth) at shorter wavelength than 250 nm. It is clear that the ZrO_2/SiO_2 samples not over 0.1 mol%-Zr has distinguishable electronic structure from the samples over 0.1 mol%-Zr. In the former samples, the zirconium oxide species would be more dispersed and interacted with silica to have Zr–O–Si linkages. This seems to be related to the high activity in photoinduced direct methane coupling (Table 1).

3.3. Phosphorescence spectra of ZrO_2/SiO_2 samples

Photoluminescence spectroscopy is a sensitive and selective to detect and investigate photoactive species [24]. Fig. 4A shows the phosphorescence emission spectra of the samples evacuated at 1073 K [18]. The wavelength of the excitation light was 300 nm. The SiO_2 sample (Fig. 4A(a)) exhibited a broad band centred around 450 nm which would be originated from surface silanols [25,26]. For the ZrO_2/SiO_2(0.01) (Fig. 4A(b)), the band maximum was shifted to around 520 nm, and some unclear shoulders similar to the fine structure were observed. The band intensity is larger than that of SiO_2, but still low and noisy. It seems that this band centred around 520 nm appeared at the expense of the band centred at 450 nm due to surface silanols. It is noted that the ZrO_2/SiO_2(0.1) (Fig. 4A(c)) exhibited a clear fine structural spectrum centred at 522 nm; the maximums observed were at 434, 454, 476, 498, 522, 549 and 581 nm. Emission intensity was highest in the present study (see the multiple factor in the figure caption). For the ZrO_2/SiO_2(0.5) samples, the fine structure became unclear and the intensity much decreased (Fig. 4A(d)). The ZrO_2/SiO_2(1.0) sample exhibited a complex band centred around 470–480 nm without fine structure (Fig. 4A(e)) which is similar to a reported spectrum of zirconium–silicon binary oxide catalyst [16].

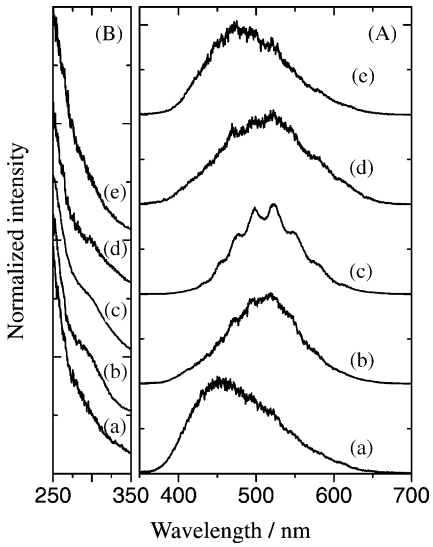

Fig. 4. Phosphorescence emission [A] and excitation spectra [B] of the samples: SiO_2 (a), ZrO_2/SiO_2(0.01) (b), ZrO_2/SiO_2(0.1) (c), ZrO_2/SiO_2(0.5) (d) and ZrO_2/SiO_2(1.0) (e). The excitation wavelength for A was 300 nm. The monitoring emission wavelength for B was 520 nm. The multiple factor for each spectrum was 13 (a), 3.1 (b), 1.0 (c), 11 (d) and 6.5 (e), respectively.

In Fig. 4B is shown the excitation spectra of these samples. The monitoring emission light was 520 nm which corresponded to the centre of the fine structural emission band. The samples of ZrO_2/SiO_2(0.01), ZrO_2/SiO_2(0.1), and ZrO_2/SiO_2(0.5) showed a shoulder band at 300 nm (Fig. 4B(b–d)). Other samples, SiO_2 (Fig. 4B(a)) and ZrO_2/SiO_2(1.0) (Fig. 4B(e)), did not exhibit such a band. These results suggest that the band in the excitation spectrum corresponds to the fine structural emission band centred around 520 nm. These mean that the photoactive sites on ZrO_2/SiO_2 samples containing moderate amount of zirconium oxide are excited by the light of around 300 nm and emit the intense and vibrational phosphorescence centred around 520 nm.

Since the fine structural spectra of the highly dispersed vanadium oxide species on silica was reported [27], the fine structure helps us to understand the structure of the photoactive sites [25–35]. The fine structure is typically due to the vibration mode of the photoexcited metal–oxygen bond in the luminescence species. In the case of TS-1 (Ti-silicate), only the samples of the low Ti content (typically 0.5 mol% of Ti) show the fine structural photoluminescence spectra [28]. Also in the case of silica–alumina [7], only isolated tetrahedral Al species in silica matrix (less than 20 mol% of Al) clearly show the fine structure on the photoluminescence spectra. In the present study, the fine structural phosphorescence spectra were observed on the samples of low zirconium content such as 0.01 and 0.1 mol% (Fig. 4A(b and c)). Thus, it is suggested that the luminescence species are the highly dispersed zirconium oxide species. An increase of Zr loading of more than 0.1 mol% reduce the emission intensity and diminished the fine structure,

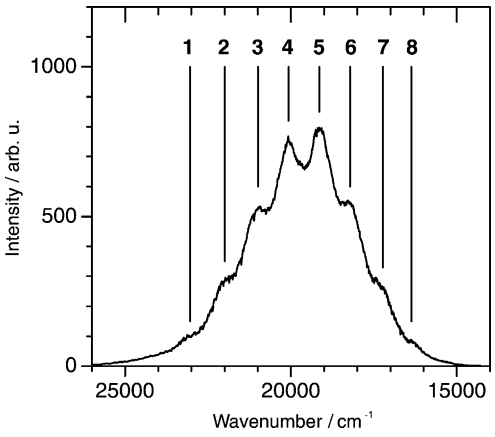

Fig. 5. The position maximum on the fine structural phosphorescence spectrum of ZrO_2/SiO_2(0.1) evacuated at 1073 K. The excitation wavelength was 300 nm. The values of maximums were listed in Table 2.

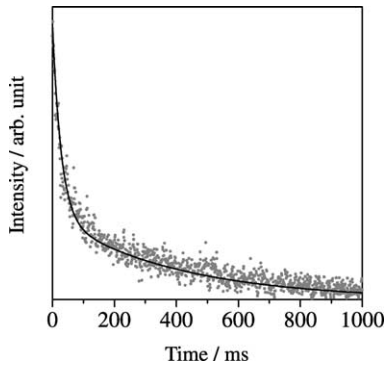

Fig. 6. Experimental (dots) and simulated (line) decay curve of phosphorescence of ZrO_2/SiO_2(0.1) evacuated at 1073 K. The excitation wavelength was 300 nm and the monitoring emission wavelength was 520 nm.

probably due to the formation of zirconium oxide aggregates at the expense of highly dispersed zirconium oxide species.

Fig. 5 shows the maximum position of the fine structure in cm^{-1} unit. Observed are eight maximums and the intervals between them correspond to the vibration energy of the photoexcited sites. The intervals seem to be almost constant. Although it seems difficult to determine the strict positions of some maximums in Fig. 5, the estimated position of the maximums and their intervals are listed in Table 2. The error in each maximum position was estimated ca. $\pm 50\,cm^{-1}$. Assuming that the intervals of vibration energy levels were constant, the vibration energy of the photoexcited sites was estimated as the average of the intervals. When the average of intervals was calculated as the mean of the middle five values ignoring the first and the last values, it was $955\,cm^{-1}$. When all seven values are used for the calculation, the average is $953\,cm^{-1}$. We employed the former value that seems to be more accurate: the vibration energy of the luminescence moiety on the ZrO_2/SiO_2(0.1) was $955\,cm^{-1}$. This value is close to that for Ti–O–Si in TS-1 ($965\,cm^{-1}$) [28] and Al–O–Si in silica–alumina ($985\,cm^{-1}$, calculated from the data in Ref. [7]), but different from that for V=O ($1040\,cm^{-1}$) [24] in VO_4 on the surface of silica. For ZrO_2–SiO_2 glasses treated at 973 K [36], broad Raman bands observed at $954\,cm^{-1}$ and an infrared band at $975\,cm^{-1}$ are assigned to Zr–O–Si linkage. Silica-supported zirconia [37] shows an infrared band at $945\,cm^{-1}$, and zirconium silicate [38] shows an infrared band at $960\,cm^{-1}$; both are attributed to the symmetric stretching vibration of the Zr–O–Si linkage. These values are in good agreement with the present value obtained from photoluminescence spectroscopy, suggesting that the photoluminescence site is Zr–O–Si linkage. Photoexcitation on the Ti–O–Si in TS-1 is explained as charge transfer from ligand oxygen to titanium (LMCT, ligand-to-metal charge transfer) [39]. On the analogy of Ti system to Zr system, it is suggested the photoexcitation occurs by charge transfer from oxygen to zirconium on the Zr–O–Si linkage of the highly dispersed zirconium oxide species in ZrO_2/SiO_2.

Since it is suggested that the photoactive sites would be the most possible candidate as the active sites for the photoinduced reaction, it is very likely that the highly dispersed zirconium oxide species exhibiting the fine structure in photoluminescence spectra are the highly active sites for the photoinduced direct methane coupling.

Table 2
The maximums and their intervals of the fine structure on the phosphorescence spectrum of ZrO_2/SiO_2(0.1)

No.[a]	Maximum		The interval to the next maximum (cm^{-1})
	nm	$\times 10^4\,cm^{-1}$	
1	434.0	2.304	1040
2	454.6	2.200	1010
3	476.4	2.099	919
4	498.2	2.007	930
5	522.4	1.914	928
6	549.0	1.821	991
7	580.6	1.722	852
8	610.8	1.637	

[a] The number corresponds that in Fig. 5.

3.4. Decay curve analysis

The variation in the phosphorescence spectra with an increase of zirconium content (Fig. 4) suggested that at least two kinds of emission sites are present on ZrO_2/SiO_2 system. This was confirmed through analyses of phosphorescence decay curves. The phosphorescence emission decay curve of ZrO_2/SiO_2(0.1) is representatively shown in Fig. 6 (dots). This decay curve was recorded with excitation light of 300 nm and monitoring emission light at 520 nm. The decay curve in Fig. 6 seems not to be described by one exponential function, exhibiting there are at least two kinds of emission sites that have different lifetime from each other.

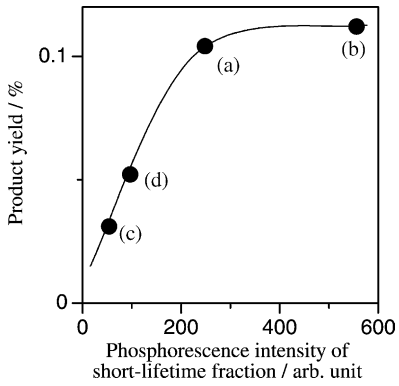

Fig. 7. A plot of product yield over the ZrO_2/SiO_2 sample in the photoinduced direct methane conversion versus calculated phosphorescence emission intensity of short-lifetime fraction. The each plot corresponds (a) ZrO_2/SiO_2(0.01), (b) ZrO_2/SiO_2(0.1), (c) ZrO_2/SiO_2(0.5), and (d) ZrO_2/SiO_2(1.0) samples.

When two kinds of emission sites are present, the decay curve is described by following equation:

$$I = I_0 \left[A_1 \exp\left(-\frac{t}{\tau_1}\right) + A_2 \exp\left(-\frac{t}{\tau_2}\right) \right] \quad (2)$$

where τ_i is a lifetime of emission, and A_i a fraction of each emission. Assuming two components exist, the experimental decay curve of ZrO_2/SiO_2(0.1) was simulated by this equation. The best-fit result is shown as a line in Fig. 6, which well simulates the experimental data. The lifetime of the major component was estimated 28 ± 5 ms, while that of the minor component was around 4×10^2 ms. This means that the phosphorescence emission sites having short-lifetime are responsible for the fine structure on the spectrum; in other words, the sites are the Zr–O–Si linkages. The decay curves of most samples seemed to consist of at least two components. Thus, the fitting analysis was also applied to other samples, and it was revealed that the major component has shorter lifetime. The lifetime of the short-lifetime component was 20–35 ms.

Fig. 7 shows a plot of the product yield versus calculated phosphorescence emission intensity of short-lifetime component (I_0A_1 in Eq. (2)) of the ZrO_2/SiO_2 samples. There is a good correlation between them. This supports that the phosphorescence emission sites having short excitation lifetime and exhibiting the fine structure on the spectrum, i.e. the Zr–O–Si linkages, would be the active sites for the photoinduced direct methane coupling. This matter is similar to the case of silica–alumina system, where the photoactive sites exhibiting the fine structural emission spectra and short-lifetime (33 ms) [26] are responsible for the photoinduced direct methane coupling [7].

The ZrO_2/SiO_2(0.01) sample exhibiting higher intensity of short-lifetime fraction showed almost the same activity for the reaction as the ZrO_2/SiO_2(0.1) sample did (Fig. 7b and c), implying that other factors than the amount of photoactive sites would be also important for the reaction. Further investigations are necessary.

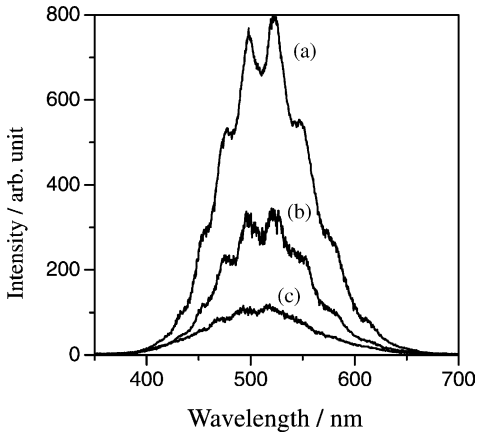

Fig. 8. Quenching effect of methane on phosphorescence emission spectra at 77 K of ZrO_2/SiO_2(0.1) evacuated at 1073 K: (a) in vacuo, (b) in the presence of methane 2.0 Torr (0.27 kPa) and (c) 3.7 Torr (0.49 kPa). Excitation wavelength was 300 nm.

3.5. Quenching effect on the phosphorescence by methane molecules

In order to obtain further supporting evidence for the active sites in this reaction, interaction between the photoactive sites and methane molecules was studied by quenching experiment. The phosphorescence emission is quenched in the presence of gaseous molecules if the molecules interact with the photoactive sites [24]. Fig. 8 shows quenching effect by methane on phosphorescence spectrum of the ZrO_2/SiO_2(0.1) sample. The intensity obviously decreased with an increase of methane pressure, indicating that methane interacted with the photoactive sites on the surface of ZrO_2/SiO_2(0.1). This suggests that the photoactive sites would be concerned with activation of methane molecules. Since the reaction did not proceed without photoirradiation, it is most likely that the photoexcited sites give the energy to the methane molecule through adsorption, or the complex of the active sites and adsorbed methane might be activated by photoenergy.

Only 2 Torr (0.27 kPa) methane introduced was enough to quench a half of the phosphorescence intensity (Fig. 8b). The quenching effect by methane was observed also in the case of silica–alumina and the quenching efficiency is almost the same as the case of silica–alumina [8], meaning that the essential performance of the photoactive sites on ZrO_2/SiO_2 is similar to those in silica–alumina system. In both cases, the photoactive sites would be the metal–O–Si linkage. They might have a common mechanism for photoexcitation and reaction.

4. Conclusions

On the ZrO_2/SiO_2 of low zirconium loading below 0.1 mol%, zirconium oxide species are highly dispersed on silica. The highly dispersed species have different local

structure from ZrO_2 particles and show a unique UV absorption band less than 350 nm. This species have Zr–O–Si linkage and exhibit the fine structure in the phosphorescence spectra. The vibration energy of the photoexcited moiety, Zr–O–Si linkage, is ca. 955 cm^{-1}.

This photoactive Zr–O–Si species can transfer the photoenergy to methane molecule and activate it. Through it, the highly dispersed zirconium species having the photoactive Zr–O–Si linkage can promote the photoinduced non-oxidative direct methane coupling at room temperature.

Acknowledgements

The X-ray absorption experiment was performed under the approval of the Photon Factory Program Advisory Committee (Proposal No. 2001G296). This work was partly supported by a Grant-in-Aid for Scientific Research on Priority Area "Catalytic Reaction Engineering toward Green Chemical Processes" from the Ministry of Education, Culture, Sports, Science and Technology (MEXT), Japan. HY acknowledges the Nitto Foundation and Japan Chemical Innovation Institute (JCII) for the financial supports.

References

[1] Y. Xu, L. Lin, Appl. Catal. A 188 (1999) 53.
[2] H.D. Gesser, N.R. Hunter, Catal. Today 42 (1998) 183, and references therein.
[3] K. Okabe, K. Sayama, H. Kusama, H. Arakawa, Chem. Lett. (1997) 457.
[4] S.L. Kaliaguine, B.N. Shelimov, V.B. Kazansky, J. Catal. 55 (1978) 384.
[5] G.N. Kuzmin, M.V. Knatko, S.V. Kurganov, React. Kinet. Catal. Lett. 23 (1983) 313.
[6] W. Hill, B.N. Shelimov, V.B. Kazansky, J. Chem. Soc., Faraday Trans. 1 (83) (1987) 2381.
[7] H. Yoshida, N. Matsushita, Y. Kato, T. Hattori, Phys. Chem. Chem. Phys. 4 (2002) 2459.
[8] H. Yoshida, Y. Kato, T. Hattori, Stud. Surf. Sci. Catal. 130 (2000) 659.
[9] Y. Kato, H. Yoshida, T. Hattori, Chem. Commun. (1998) 2389.
[10] Y. Kato, H. Yoshida, T. Hattori, Micropor. Mesopor. Mater. 51 (2002) 223.
[11] Y. Kato, N. Matsushita, H. Yoshida, T. Hattori, Catal. Commun. 3 (2002) 99.
[12] P. Pichat, J.-M. Herrmann, J. Disdier, M.-N. Mozzanega, J. Phys. Chem. 83 (1979) 3122.
[13] J.A. Navío, G. Colón, Stud. Surf. Sci. Catal. 82 (1994) 721.
[14] K. Sayama, H. Arakawa, J. Phys. Chem. 97 (1993) 531.
[15] J.A. Navío, G. Colón, M. Macías, P.J. Sánchez-Soto, V. Augugliaro, L. Palmisano, J. Mol. Catal. A 109 (1996) 239.
[16] S.C. Moon, M. Fujino, H. Yamashita, M. Anpo, J. Phys. Chem. B 101 (1997) 369.
[17] H. Yoshida, C. Murata, T. Hattori, J. Catal. 194 (2000) 364.
[18] H. Yoshida, M.G. Chaskar, Y. Kato, T. Hattori, Chem. Commun. (2002) 2014.
[19] M. Nomura, A. Koyama, KEK Report 89-16, 1989, p. 1.
[20] F.W. Lytle, R.B. Greegor, D.R. Sandstrom, E.C. Marques, J. Wong, C.L. Spiro, G.P. Huffman, F.E. Huggins, Nucl. Instrum. Meth. 226 (1984) 542.
[21] G. Mountjoy, D.M. Pickup, R. Anderson, G.W. Wallidge, M.A. Holland, R.J. Newport, M.E. Smith, Phys. Chem. Chem. Phys. 2 (2000) 2455.
[22] Y. Inaki, H. Yoshida, T. Hattori, J. Phys. Chem. B 104 (2000) 10304.
[23] Y. Inaki, H. Yoshida, T. Yoshida, T. Hattori, J. Phys. Chem. B 106 (2002) 9098.
[24] M. Anpo, M. Che, Adv. Catal. 44 (2000) 119, and references therein.
[25] Y. Kato, H. Yoshida, T. Hattori, Phys. Chem. Chem. Phys. 2 (2000) 4231.
[26] H. Yoshida, T. Tanaka, T. Funabiki, S. Yoshida, J. Chem. Soc., Faraday Trans. 90 (1994) 2107.
[27] A.M. Gritscov, V.A. Shvets, V.B. Kazansky, Chem. Phys. Lett. 35 (1975) 511.
[28] A.S. Soult, D.D. Pooré, E.I. Mayo, A.E. Stiegman, J. Phys. Chem. B 105 (2001) 2687.
[29] M. Anpo, I. Tanahashi, Y. Kubokawa, J. Phys. Chem. 84 (1980) 3440.
[30] M. Iwamoto, H. Furukawa, K. Matsukami, T. Takenaka, S. Kagawa, J. Am. Chem. Soc. 105 (1983) 3719.
[31] M. Anpo, Y. Kubokawa, J. Phys. Chem. 88 (1984) 5556.
[32] M. Anpo, N. Aikawa, Y. Kubokawa, M. Che, C. Louis, E. Giamello, J. Phys. Chem. 89 (1985) 5017.
[33] M.F. Hazenkamp, G. Blasse, J. Phys. Chem. 96 (1992) 3442.
[34] T. Tanaka, H. Yoshida, K. Nakatsuka, T. Funabiki, S. Yoshida, J. Chem. Soc., Faraday Trans. 88 (1992) 2297.
[35] H. Yoshida, T. Tanaka, A. Satsuma, T. Hattori, T. Funabiki, S. Yoshida, Chem. Commun. (1996) 1153.
[36] S.W. Lee, R.A. Condrate Sr., J. Mater. Sci. 23 (1988) 2951.
[37] Z. Dang, B.G. Anderson, Y. Amenomiya, B.A. Morrow, J. Phys. Chem. 99 (1995) 14437.
[38] B. Rakshe, V. Ramashe, V. Ramaswamy, A.V. Ramaswamy, J. Catal. 163 (1996) 501.
[39] S. Bordiga, S. Colucia, C. Lamberti, L. Marchese, A. Zecchina, F. Boscherimi, F. Buffa, F. Genomi, G. Leofanti, G. Petrini, G. Vlaic, J. Phys. Chem. 98 (1994) 4125.